Superthermal electron energy interchange in the ionosphere-plasmasphere system

G. V. Khazanov,[1] A. Glocer,[1] M. W. Liemohn,[2] and E. W. Himwich[1]

Received 10 September 2012; revised 10 January 2013; accepted 12 January 2013.

[1] A self-consistent approach to superthermal electron (SE) transport along closed field lines in the inner magnetosphere is used to examine the concept of plasmaspheric transparency, magnetospheric trapping, and SE energy deposition to the thermal electrons. The dayside SE population is generated both by photoionization of the thermosphere and by secondary electron production from impact ionization when the photoelectrons collide with upper atmospheric neutral particles. It is shown that a self-consistent approach to this problem produces significant changes, in comparison with other approaches, in the SE energy exchange between the plasmasphere and the two magnetically conjugate ionospheres. In particular, plasmaspheric transparency can vary by a factor of two depending on the thermal plasma content along the field line and the illumination conditions of the two conjugate ionospheres. This variation in plasmaspheric transparency as a function of thermal plasma and ionospheric conditions increases with *L*-shell, as the field line gets longer and the equatorial pitch angle extent of the fly-through zone gets smaller. The inference drawn from these results is that such a self-consistent approach to SE transport and energy deposition should be included to ensure robustness in ionosphere-magnetosphere modeling networks.

Citation: Khazanov, G. V., A. Glocer, M. W. Liemohn, and E. W. Himwich (2013), Superthermal electron energy interchange in the ionosphere-plasmasphere system, *J. Geophys. Res.: Space Physics.*, *118*, doi:10.1002/jgra.50127.

1. Introduction

[2] It is generally recognized that there is a need to better understand the coupling processes between inner magnetospheric plasma populations, fields, and regions. Self-consistent calculations, including global modeling that links the inner magnetosphere to other regions of geospace, must continue to be developed to provide a global forecast of the space plasma environment. In addition, improvements are needed to correctly describe of the different populations in inner magnetosphere, keeping in mind the applicability of the different sets of transport equations involved in the corresponding self-consistent coupling loop.

[3] Among such populations are the superthermal electrons (SEs), which are the major energy contributors, via Coulomb collisional processes, to the ionosphere and inner plasmasphere [see *Khazanov et al.*, 2000, and references therein]. SE escape from the ionosphere to the plasmasphere is controlled by strong Coulomb coupling with the thermal plasma distribution along the entire length of the magnetic field line. The plasma distribution along the field line, in turn, is controlled by electron and ion temperature distributions that are mostly determined by SE heating of the thermal electrons [*Khazanov*, 2011]. *Khazanov et al.* [1984] originally recognized the need for such self-consistent SE coupling with the thermal plasma of the inner magnetosphere when considering the plasmaspheric refilling process. Very recent studies by *Varney et al.* [2012] also recognized this need and coupled photoelectron calculations with the SAMI2 code developed by *Huba et al.* [2000] to study the energy deposition processes of photoelectrons at the low-latitude station of Jicamarca, over a range of altitudes from 90 to 1650 km ($L = 1.26$).

[4] One of the first observations of conjugate photoelectrons was by *Peterson et al.* [1977], who noted SE fluxes in the ionosphere before the satellite crossed the terminator onto the dayside. Several other studies [e.g., *Woods et al.*, 2003; *Richards and Peterson*, 2008] place an observational constraint on the amount of SE trapping within the magnetosphere as well as on the amount of SE backscatter from the conjugate ionosphere traveling back toward the original ionosphere.

[5] Previous numerical calculations have explored the relationship between SE escape from the dayside ionosphere and their scattering and energy deposition to the thermal electron population within the magnetospheric segment of the field line. Original efforts to include the magnetospheric flight of photoelectrons along closed field lines between conjugate ionospheres were conducted with the field line interhemispheric plasma (FLIP) model [*Young et al.*, 1980]. This code solves a two-stream equation for SE transport within the two conjugate ionospheres and then applies an efficiency factor

[1]Goddard Space Flight Center, National Aeronautics and Space Administration, Greenbelt, Maryland, USA.
[2]University of Michigan, Ann Arbor, Michigan, USA.

Corresponding author: A. Glocer, Goddard Space Flight Center, National Aeronautics and Space Administration, Greenbelt, MD 20771, USA. (alex.glocer-1@nasa.gov)

©2013. American Geophysical Union. All Rights Reserved.
2169-9380/13/jgra.50127

to account for plasmaspheric energy loss as the SE move through the magnetosphere between the two ionospheres. The energy lost by the SE was considered as a source term for thermal electron magnetospheric heat flux back into the topside ionosphere. This model was used in numerous studies [e.g., *Richards et al*., 1983; *Newberry et al*., 1989; *Buonsanto et al*., 1997; *Liemohn et al*., 2004] to quantify energy input to the thermal plasma from energetic particle populations in the inner magnetosphere.

[6] The two-stream transport code was originally developed for photoelectron fluxes at Earth more than 40 years ago by *Banks and Nagy* [1970] and *Nagy and Banks* [1970]. Since that time, it was routinely used by many studies to examine SE transport in both Earth and planetary ionospheres. *Richards and Peterson* [2008] carry on the two-stream code legacy in a very recent study by showing an excellent comparison of calculated backscattered photoelectron fluxes in the dark ionosphere with corresponding FAST satellite data. As was pointed out by *Lejeune* [1978] many years ago in his paper, ". . .the two-stream calculation can give accurate results in any case, if angular distribution is not requested, when one *chooses* the mean pitch-angle cosine equal to 0.5 or 0.577, instead of 3/8 originally chosen by *Nagy and Banks* [1970]". We italicized the word "chooses" here because this is an intrusion in the physical formalism of the two-stream code. Note, however, that the two-stream "formalism" is mostly phenomenological and cannot be derived starting from the first principles of plasma kinetic theory. In later usage of two-stream code by *Newberry et al*. [1989], a comparison was made between data from the retarding ion mass spectrometer on the Dynamics Explorer 1 (DE 1) satellite and the FLIP model. In this case, the FLIP model included a phenomenological factor (trapping factor) to represent the amount of energy lost to the plasmasphere from the photoelectrons, and the study concluded that good agreement between the calculated and measured ion temperatures is achieved when approximately 55% of the total photoelectron flux is trapped in the plasmasphere. Contrary to this conclusion, *Richards and Peterson* [2008] found "that photoelectrons are able to travel the long journey from the sunlit hemisphere to the satellite without significant degradation indicating that pitch-angle scattering and trapping of photoelectrons in the magnetosphere may be small." This statement, however, contradicts the 55% SE energy trapping discussed by *Newberry et al*. [1989] that conformed to the rigorous kinetic SE calculations by *Khazanov and Liemohn* [1995].

[7] *Khazanov et al*. [1994] developed a numerical formulation for simulating SE transport along a closed field line, and *Khazanov and Liemohn* [1995] expanded this into both a numerical model and phenomenological model of SE interplay within the ionosphere-plasmasphere system. *Liemohn and Khazanov* [1995] conducted a systematic study quantifying the heating rates imparted to the thermal electrons along the field line, which was followed by the more general study of *Khazanov and Liemohn* [2000], that placed the photoelectron heating rates in the context of other midlatitude energy sources to the thermal plasma. A more global approach to SE transport within the inner magnetosphere was used by *Khazanov et al*. [1996, 1998], who applied a bounce-averaged kinetic equation model to the problem of SE fluxes and energy deposition. *Khazanov et al*. [2000] and *Khazanov and Liemohn* [2002] further explored the day-to-night SE transport and the SE energy deposition to thermal plasma relative to other energy sources.

[8] Because of the interconnection between the ionospheric source and the plasmaspheric trapping and storage of SE, we have developed a comprehensive kinetic theory of SE transport that is equally valid in the ionosphere and in the plasmasphere and that self-consistently couples the conjugate magnetospheric hemispheres [*Khazanov et al*. 1994; *Khazanov*, 2011]. It has been shown in these studies that such a self-consistent approach produces significant changes in the SE distributions compared with "pure" ionospheric or plasmaspheric calculations and must be included in a future ionosphere-magnetosphere modeling network. This paper continues the aforementioned studies and focuses on the ionosphere-plasmasphere energy interchange, specifically the SE flux escaping from the ionosphere to the conjugate region. In this paper, we decided to discuss the only one aspect of the two-stream application: the ionosphere-plasmasphere transport of photoelectrons. Our conclusions, however, are equally valid for the secondary electrons that are produced by precipitation of the high energy electrons of magnetospheric origin.

2. SE Model

[9] The starting point of our SE ionosphere-plasmasphere coupling study for energies $E > 1$–2 eV is the following field-aligned, guiding-center kinetic equation [*Khazanov*, 2011]

$$\frac{\beta}{\sqrt{E}}\frac{\partial\phi}{\partial t} + \mu\frac{\partial\phi}{\partial s} - \frac{1-\mu^2}{2}\left(\frac{1}{B}\frac{\partial B}{\partial s} - \frac{F}{E}\right)\frac{\partial\phi}{\partial\mu} + EF\mu\frac{\partial}{\partial E}\left(\frac{\phi}{E}\right) = Q + \bar{S} \quad (1)$$

[10] This equation determines the differential number flux distribution ϕ in along a magnetic flux tube in gyration-averaged phase space. The independent variables are time t, the distance s along the field line, kinetic energy E of the electrons, and cosine of the local pitch angle $\mu = \cos\alpha$. Other forces, for instance the electric fields, are included in F. The inhomogeneity of the geomagnetic field ($\partial B/\partial s$) is also accounted for. Q represents the source of electron population due to two illumination sources: direct solar illumination and scattered light illumination. The equation also accounts for elastic and inelastic scattering with upper atmospheric neutrals as well as with thermal electrons and ions along the entire flux tube. Those collisions are represented by the $\bar{S}$ term in equation (1). For full details regarding $\bar{S}$, see *Khazanov* [2011]. We note that the collision term $\bar{S}$ also includes the production of secondary (tertiary, etc.) electrons in the upper atmosphere. As a result, the resulting differential number flux distributions represent the total electron spectra.

[11] The results presented are determined by a solution to the kinetic equation along a closed magnetic field line. Moreover, it is solved at the same time for the two conjugate ionospheres as well as the plasmasphere. The advantage of this unified approach is that no artificial boundaries are introduced between the ionosphere and the magnetosphere during the determination of the SE distribution along the complete length of the field line. Avoiding such artificial boundaries sidesteps uncertainties introduced by specifying these boundary conditions explicitly. The solution to the kinetic equation

completely accounts for backscattered electrons and treats the "loss cone" and "trapped zone" photoelectron populations together rather than separately. This approach is applicable to arbitrary illumination conditions.

[12] To perform the calculations as well as benchmarking our results with all our previous calculations, we used the following input for our SE model. The *Hinteregger* [1981] model provided Solar EUV and X-ray radiation spectra, and the MSIS-90 model [*Hedin*, 1991] provided the neutral thermospheric densities and temperatures. The IRI model [*Bilitza*, 1990] provided the field-aligned thermal electron density information in the ionosphere. That solution was extended to plasmasphere by assuming that the thermal electron density n_e in the plasmasphere is proportional to the geomagnetic field strength B. Specifically, we made two such assumptions: $n_e \sim B$, corresponding to a filled plasmasphere [*Newberry et al.*, 1989]; and $n_e \sim B^2$, indicating an intermediate step during plasmaspheric refilling [*Khazanov et al.*, 1984). The photoabsorption and photoionization cross sections for O, O_2, and N_2 are provided by *Fennelly and Torr* [1992]. O_2 and N_2 partial photoionization cross sections are from *Conway* [1988]. The partial photoionization cross sections for O are taken from *Bell and Stafford* [1992]. Elastic scattering cross sections as well as state-specific excitation and ionization are from *Solomon et al.* [1988]. The calculations were all performed for noon mangetic local time (MLT) at equinox, with $F_{10.7}$ and $<F_{10.7}>$ values of 150, which indicate symmetric conditions in the conjucate atmospheres with typical solar radiation intensity levels.

[13] We note that the use of new Solar EUV and X-ray radiation spectra data—like those obtained, for example, by the *Chamberlin et al.* [2007, 2008] model—will not change the conclusions that are derived from our results below.

3. SE Escape Into the Plasmasphere

[14] SE motion in the inhomogeneous geomagnetic field and Coulomb collisions with the background thermal plasma are the two primary processes controlling the behavior of SE in the plasmasphere. (Note that the two-stream model neglects the divergence of the geomagnetic field.) Direct observations by *Galperin and Mulyarchik* [1966] indicated that the motion of SE in the plasmasphere is subject to collisions. This is true although the mean free path of SEs significantly surpasses the characteristic spatial scale of the thermal plasma density along the geomagnetic field line. Some qualitative discussion of electron trapping and the associated plasmaspheric heating was provided by *Sanatani and Hanson* [1970] and *Nagy and Banks* [1970]; however, *Gastman* [1973], *Takahashi* [1973], and *Lejeune and Wormser* [1976] provided the first attempts at quantitative calculations. In this section, we will demonstrate, based on theoretical considerations, the importance of pitch angle diffusion due to Coulomb collisions to SE transport in the plasmasphere.

[15] The kinetic Boltzmann equation for the SE above 1000 km is given by [*Khazanov*, 2011]:

$$\mu\frac{\partial f}{\partial s}+\frac{1-\mu^2}{2\sigma}\frac{\partial\sigma}{\partial s}\frac{\partial f}{\partial\mu}=\frac{A n_e}{E^2}\left\{E\frac{\partial f}{\partial E}+\frac{\partial}{2\partial\mu}\left[\left(1-\mu^2\right)\frac{\partial f}{\partial\mu}\right]\right\}, \quad (2)$$

where μ is the cosine of the pitch angle, $f = \Phi/E$ is the distribution function of the SE, Φ is the flux of the electrons, E is the energy of the electrons, and $\sigma(s) = B(s_0)/B(s)$, where $B(s_0)$ and $B(s)$ are the magnetic field intensities at the boundary between the ionosphere and plasmasphere and a distance s along a given field line, respectively. We choose appropriate values at the boundaries for a given calculation. The terms on the left-hand side of equation (2) describe changes to the SE distribution due to motion in an inhomogeneous magnetic field. The terms on the right-hand side describe changes in energy and pitch angle resulting from collisions with the thermal plasma. The second term on the right-hand side of equation (2) describes the pitch-angle diffusion. This term is only indirectly included in the SE transport two-stream formulation as a backscatter probability, based on pitch angle diffusion rates. Furthermore, this term is only used in the ionosphere, whereas in the plasmasphere the two-stream approach simply applies a chosen or data-fitted trapping efficiency attenuation factor. The inclusion or magnitude of this term seems to depend on the particular study. *Richards and Peterson* [2008] indicate that pitch-angle diffusion in their study was negligible, whereas the term was found to be quite significant in the study by *Newberry et al.* [1989]. As shown below, pitch-angle diffusion plays a very important role in the plasmasphere compared with the first term on the right-hand side of equation (2) that represents SE energy losses.

[16] In the simplified case where collisions are neglected and the ionosphere is the only source of electrons, the distribution function at the foot of the field line (s_0) uniquely determines the solution at every point along the line. This is due to conservation of the first adiabatic invariant. The cosine of the pitch angle, μ, at any particular point, s, along the field line can be related to its value at the base (s_o), written as μ_{s0}, and can be expressed by

$$\mu_{s0} = \sqrt{1-\sigma(s)\left(1-\mu^2\right)} \quad (3)$$

[17] Given that μ_{s0} is real, the pitch angle a point s is bounded by

$$1-\frac{1}{\sigma(s)} \le \mu^2 \le 1 \quad (4)$$

[18] The inequality described in equation (4) defines a family of possible trajectories in the (s,μ) plane. These solutions correspond to region I, as shown in Figure 1. Figure 1 illustrates how the pitch angle becomes more field aligned as the electrons traverse the distance from the ionosphere toward the magnetic equator and then becomes more perpendicular as they approach the conjugate ionosphere. Particles corresponding to this region can move freely between conjugate hemispheres and are denoted as "precipitating," "free," or "fly-through" electrons.

[19] Electrons that are trapped by the geomagnetic field are defined by the following:

$$\mu^2 \le 1-\frac{1}{\sigma(s)} \quad (5)$$

Such particles are represented by region II in Figure 1 and move in the (s, μ) space in closed paths, along trajectories, L_{II}. The reflection points, s_{ref}, are uniquely determined by

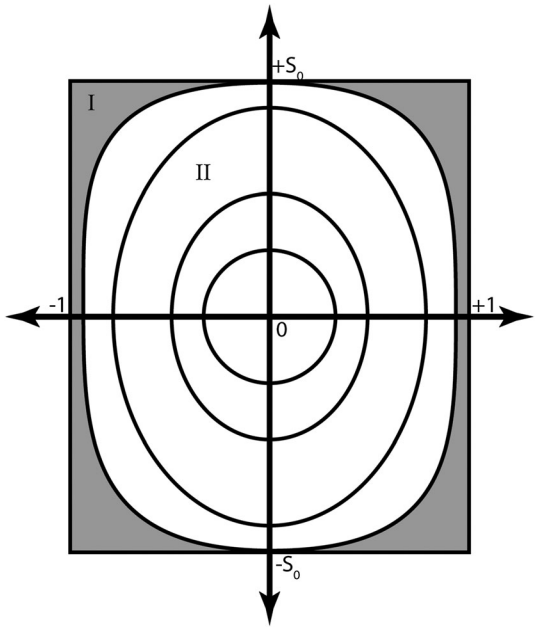

Figure 1. Illustration of the trapped or capture {II} and precipitation "fly-through" {I} zones in the *s-m* plane (white and shaded regions, respectively). The solid lines are representative trajectories of trapped electrons.

the value of the pitch angle cosine, μ_0, at the equator($s = 0$), which is

$$\mu_0 = \frac{\mu}{|\mu|}\sqrt{1 - \frac{\sigma(s)}{\sigma_0}(1-\mu^2)}, \tag{6}$$

where $\sigma_0 = \sigma(0) = B(s_0)/B(0)$. Likewise, we can use the condition $\mu = 0$ to find the reflection point as follows:

$$\sigma(s_{\mathrm{ref}}) = \sigma_o\left(1 - \mu_0^2\right). \tag{7}$$

[20] When collisions are neglected, the populations in the trapped and fly-through regions are independent because there are no collisions to facilitate the exchange of particles between the trapped and fly-through regions. The trapped electron population is therefore a consequence of direct SE production in this zone. These sources are extremely small in the plasmasphere, and it is thus reasonable to assume that $f_{\mathrm{II}} = 0$. In this case, the thermal electron heating rate due to these SEs for any position along the field line can be expressed as [*Khazanov*, 1979]:

$$Q_e = Q_e(s = \pm s_o)\left[1 - \sqrt{1 - 1/\sigma(s)}\right]. \tag{8}$$

We assumed in this derivation that the SE flux is isotropic at the base of the field line and that the integration over μ took into account inequality (5).

[21] The preceding analysis completely neglected the effects of collisions in the plasmasphere; accounting for those collisions significantly changes the final result. This is true even in the case that the mean free path of the SEs $\lambda \sim E^2/An_e$ is greater than the characteristic length of the field line $H_\sigma \sim \sigma/\mathrm{d}\sigma/\mathrm{d}s$. We demonstrate this fact by examining the pitch angle diffusion, represented in the second term on the right of equation (2),

$$\frac{\mathrm{An}_e}{2E^2}\frac{\partial}{\partial\mu}\left[\left(1-\mu^2\right)\frac{\partial f}{\partial\mu}\right] \sim \frac{\mathrm{An}_e}{E^2}\frac{f}{\Delta\mu}, \tag{9}$$

where $\Delta\mu$ is the width of the fly-through zone at $s = 0$ ($\sigma = \sigma_0$). The value of $\Delta\mu$ can be written as

$$\Delta\mu = 1 - \mu_{\mathrm{ob}}, \tag{10}$$

where μ_{0b} corresponds to that pitch angle at the equator which results in reflection at $s = s_{\mathrm{o}}$. Equation (10) can be evaluated by using equation (7) and recognizing the fact that μ_{0b} is close to unity, giving

$$\Delta\mu \approx \frac{1}{2\sigma_o}. \tag{11}$$

Putting equation (11) back into equation (9) demonstrates that pitch angle diffusion alters the distribution function over a length scale of $\lambda/2\sigma_0 \sim H_\sigma$. Because $\sigma_0 \gg 1$ for mid- and high-latitude field lines, we must account for pitch angle diffusion even when the mean free path is much greater than the characteristic length of a field line. A clear way to understand this result is to notice that the pitch angle width of region I is extremely narrow near the equatorial plane. Therefore, even small angle deflections will result in electron trapping. This result, as we pointed out earlier, is completely missing in the two-stream code formulation.

4. The Phenomenology of SE Ionosphere-Plasmasphere Transport

[22] Let us continue with a qualitative discussion of SE transport in the ionosphere-plasmasphere system. Following *Khazanov* [2011], we introduce the following quantities: ε is the fraction of SE lost in the plasmasphere; β is the part of SE energy returned from the plasmasphere due to the electron scattering into the loss cone; $\alpha = 1 - \varepsilon - \beta$ is the "pure" part of plasmaspheric transparency; and A_1 and A_2 are the SE albedos of each ionosphere, respectively, in its conjugate hemisphere. The plasmaspheric transparency is defined as the ratio of the number of particles leaving one end of a magnetic flux tube to the number of particles entering at the other end,

$$T(E) = \frac{\int_{\mu_0 B}^{1} \mu_0 \Phi(E, \mu_0, , s_1) d\mu_0}{\int_{\mu_0 B}^{1} \mu_0 \Phi(E, \mu_0, -s_1) d\mu_0}, \quad \mu_0 \frac{\mu}{|\mu|}\sqrt{1 - \frac{B_0}{B}(1-\mu^2)} \tag{12}$$

Here, s_1 is the ionosphere-plasmasphere boundary altitude, taken to be 800 km in the present study, B_0 and μ_0 denote the magnetic field and the cosine of the pitch-angle at the magnetic equator of the flux-tube, respectively, and $\mu_{0B} = \sqrt{1 - B_0/B(s)}$ is the loss cone boundary.

[23] Previous studies of "pure" plasmaspheric SE transport demonstrated that transparency has strong dependence on a parameter proportional to the Coulomb cross section and to the complete thermal electron content in a magnetic flux tube

[*Takahashi*, 1973; *Lejeune and Wormser*, 1976; *Krinberg and Matafonov*, 1978; *Khazanov et al.*, 1992]. Given that processes such as diffusion into the trapped region, reflections resulting from elastic collisions with neutral and charged particles in the ionosphere, and the redistribution of the flux at low energies due to interactions with neutral and charged particles are included in equation (1) enables plasmspheric "transparency" to recover its traditional definition (12) [*Khazanov et al.*, 1994].

[24] Figure 2 is a schematic of the ionosphere-plasmasphere system along a closed field line of the inner magnetosphere. At the interface between the first ionosphere (on the left) and the magnetospheric segment of the field line, two hemispheric fluxes can be defined: an upward SE flux escaping from the ionosphere, denoted by F_1^+, and a downward SE flux precipitating into the ionosphere, F_1^-. A similar pair of fluxes can be defined in the second ionosphere (on the right), with the upward escaping SE flux denoted by F_2^- and the downward precipitating SE flux defined as F_2^+. The definitions are chosen such that the two "+" fluxes are in the same direction and the two "−" fluxes are flowing in the opposite direction along the field line.

[25] By taking into account multiple reflections in the ionosphere and plasmasphere, the unidirectional fluxes F_1^+, F_2^+ at the boundaries of the ionosphere and plasmasphere can be presented in the form

$$F_1^+ = F_{01}^+\left[1 + \alpha^2 A_1 A_2 + (a^2 A_1 A_2)^2 + \ldots + \beta A_1 + (\beta A_1)^2 \ldots\right] + \\ + F_{02}^- \alpha A_1 \left[1 + \alpha^2 A_1 A_2 + (a^2 A_1 A_2)^2 + \ldots + \beta A_1 + (\beta A_1)^2 \ldots\right] = \\ = \left(F_{01}^+ + F_{02}^- \alpha A_1\right)\left[\left(1 - \alpha^2 A_1 A_2\right)^{-1} + \beta A_1/(1 - \beta A_1)\right] \tag{13}$$

$$F_2^- = \left(F_{02}^- + F_{01}^+ \alpha A_2\right)\left[\left(1 - \alpha^2 A_1 A_2\right)^{-1} + \beta A_2/(1 - \beta A_2)\right], \tag{14}$$

$$F_2^+ = \alpha F_1^+ + \beta F_2^-, \qquad F_1^- = \alpha F_2^+ + \beta F_1^+. \tag{15}$$

Here, F_{01}^+ and F_{02}^- are the fluxes entering the plasmasphere from the local ionospheres. These particles are generated in the ionosphere by photoionization or impact ionization processes.

[26] Using equations (13)–(15), we can now derive an expression for the fluxes that are escaping from the ionosphere to the plasmasphere and plasmaspheric transparency $T = F_2^+/F_1^+$. In particular, we can use these expressions to find the phenomenalogical coeficients by considering limiting cases: symmetic conditions of illumination, asymetric conditions of illumination with no SE source in the second ionosphere, and asymetric conditions of illumination with no backscattering in the unilluminated ionosphere. Moreover, consideration of these limiting cases will demonstrate that the transparency is only rarely dependent on the pure part of the transparency alone but is often also dependent on other aspects of ionosphere-plasmasphere coupling.

[27] When we have symmetric conditions of illumination in the conjugate hemispheres ($F_{01}^+ = F_{02}^- = F_0$, and $A_1 = A_2 = A$), these quantities can be presented as

$$F_1^+ = F_0(1 + \alpha A)\left(\left(1 - \alpha^2 A^2\right)^{-1} + \beta A/(1 - \beta A)\right) \tag{16}$$

$$F_2^+ = (\alpha + \beta)F_1^+; \quad F_2^- = F_1^+; F_1^- = F_2^+ \tag{17}$$

$$T_1 = \alpha + \beta = 1 - \varepsilon \tag{18}$$

[28] We consider a second scenario with no source of SE in the second ionosphere $\left(F_{02}^- = 0, F_{01}^+ = F_0, A_1 = A_2 = A\right)$:

$$F_1^+ = F_0\left(\left(1 - \alpha^2 A^2\right)^{-1} + \beta A/(1 - \beta A)\right) \tag{19}$$

$$F_2^+ = \alpha(1 + \beta A)F_1^+; \quad F_2^- = \alpha A F_1^+; \quad F_1^- = \left(\alpha^2 A + \beta\right)F_1^+ \tag{20}$$

$$T_2 = \alpha(1 + \beta A). \tag{21}$$

[29] Finally, we consider a case with no backscattering in the unilluminated ionosphere ($F_{02}^- = 0$ and $A_2 = 0$):

$$F_1^+ = F_0(1 + \beta A/(1 - \beta A)); \quad F_2^+ = \alpha A F_1^+; \\ F_2^- = 0; \quad F_1^+ = \beta F_1^+ \tag{22}$$

$$T_3 = \alpha. \tag{23}$$

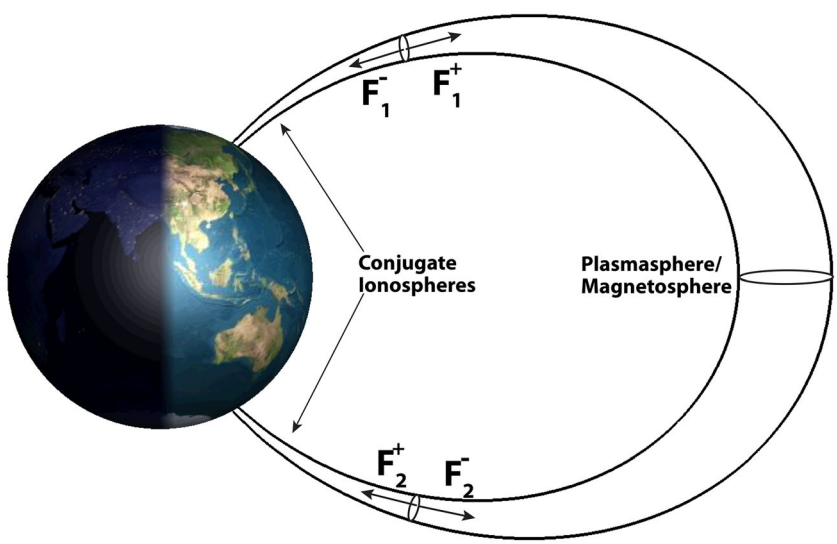

Figure 2. Schematic of SE flux definitions in the ionosphere-plasmasphere system.

[30] Equations (16)–(23) demonstrate that ionosphere-plasmasphere coupling processes determine the SE fluxes. The quantity T is not identical to the "pure" part of the plasmaspheric transparency α; rather, it can be smaller or, more often, larger than α due to pitch angle scattering and energy degradation within the magnetospheric segment of the field line.

5. Results and Discussion

[31] The two-stream calculation and our approach have different theoretical underpinnings and different representations of the physical processes underlying SE transport. Therefore, we use the phenomenological model described in section 4 to compare these formalisms and assess the importance of including different physical processes by determining coefficients appropriate to each model. For our kinetic calculations described in section 2, the coefficients are found by considering limiting cases, and their associated equations in the section 4. We also use the same approach to compare our results with the rigorous SE kinetic studies presented by *Krinberg and Matafonov* [1978] that had been performed using some simplifications in the calculations of the plasmaspheric transparency.

[32] The solution of the kinetic equation (1) allows us to determine the plasmaspheric transparency as defined by equation (12) and based on equations (18), (21), and (23) to find several quantities: the "pure" plasmaspheric transparency ($<\alpha>$); the part of SE energy reflected from the plasmasphere to the source ionosphere ($<\beta>$); and atmospheric albedo ($<A>$). The angle brackets denote integration over the energy range of 1–125 eV. This represents the most active SE energy range that provides approximately 100% of the energy deposition to the thermal electrons in the plasmasphere. Using the relation $<\alpha>+<\varepsilon>+<\beta>=1$, we also can find $<\varepsilon>$, the fraction of energy trapped within and lost to the plasmasphere. Such calculations are presented in Table 1 for the different L-shells and plasma distributions along the field lines with omission of the angle brackets. For simplicity, we also have omitted all these angle brackets below, remembering that we deal with all parameters integrated over the energy range of 1–125 eV.

[33] As follows from Table 1, the amount of the *total* energy that is redistributed inside of the ionosphere-plasmasphere system can vary greatly. This variation depends on several factors, most notably the conditions of illumination and reflection in the conjugate ionospheres, the L-shell of the magnetic field line (which determines the path length through the magnetosphere) and the plasma distribution along the geomagnetic field line. Approximately 25%–60% of the SE energy escaping from the ionosphere is carried all the way into the conjugate ionosphere, and only approximately 20% is returned to the original ionospheric region. The rest of the energy, approximately 25%–60%, is deposited to the plasmaspheric thermal electrons. This trapped energy is absorbed by the thermal electron and eventually returns to the conjugate ionospheres as a magnetospheric energy flux carried by the core electrons.

Table 1. Calculated Parameters

L	T1	T2	T3 = α	β	ε	A	$\hat{A}$
$L=2$, $n_e \sim B$	0.631	0.515	0.455	0.177	0.368	0.753	0.665
$L=3$, $n_e \sim B$	0.522	0.384	0.339	0.182	0.478	0.728	0.642
$L=L=4$, $n_e \sim B$	0.485	0.337	0.295	0.190	0.515	0.738	0.647
$L=5$, $n_e \sim B$	0.437	0.284	0.249	0.188	0.562	0.735	0.645
$L=6$, $n_e \sim B$	0.405	0.247	0.217	0.188	0.595	0.732	0.643
$L=2$, $n_e \sim B^2$	0.779	0.687	0.609	0.170	0.220	0.752	0.667
$L=3$, $n_e \sim B^2$	0.743	0.640	0.571	0.171	0.257	0.701	0.626
$L=4$, $n_e \sim B^2$	0.748	0.639	0.572	0.176	0.252	0.663	0.594
$L=5$, $n_e \sim B^2$	0.733	0.621	0.559	0.174	0.266	0.632	0.569
$L=6$, $n_e \sim B^2$	0.726	0.610	0.551	0.174	0.274	0.606	0.548

[34] Now let us discuss the backscatter process by the dark thermosphere. The coefficient A, defined earlier as an ionospheric albedo, represents the probability of the SEs scattering back to the plasmasphere and conjugate region of the ionosphere. To deal with the backscatter coefficient of the dark ionosphere, we go to our phenomenological SE model presented in the previous section and define a backscatter coefficient, $\hat{A}$, based on the fluxes F_2^+ and F_2^- that are determined by equation (16) and take into account ionosphere-plasmasphere SE coupling processes. In this case, $\hat{A} = F_2^-/F_2^+$ (new expression for the albedo) can be presented as

$$\langle \hat{A} \rangle = \langle A \rangle (1 + \langle \beta \rangle \langle A \rangle)^{-1} \tag{24}$$

As follows from parameter values presented in Table 1, the ionosphere-plasmasphere SE coupling processes have a noticeable influence on a total ionospheric backscatter. The value of this coefficient, $\hat{A}$, is comparable with the results of the FAST measurements and the calculation by *Richards and Peterson* [2008], showing that approximately 55%–60% of the precipitating flux energy is backscattered from the thermosphere back to the conjugate hemisphere.

[35] We can now evaluate how SE ionosphere-plasmasphere coupling processes contribute to the formation of SE integrated fluxes at the boundaries of the ionosphere and plasmasphere. Figures 3 and 4 present results that are calculated for the symmetric and nonsymmetric conditions of illumination in the conjugate ionospheric regions and are based on equations (16)–(21) of the SE phenomenological model discussed in the previous section. These plots show the normalized energy fluxes flowing out of (and into) the first ionosphere $\left(F_1^{\pm}/F_0\right)$ and out of (and into) the second ionosphere $\left(F_2^{\pm}/F_0\right)$. Here, we also consider different thermal plasma density distributions along the geomagnetic field lines, with the left half of the figure calculated for $n_e \sim B$, and the right half of the figure calculated for $n_e \sim B^2$, which is more appropriate for conditions during the refilling of depleted flux tubes.

[36] For each L-shell, we present results from three different cases of SE flux calculations that are characterized by the influence of different ionosphere-plasmasphere processes. In both figures, each of these cases, with different included factors in the flux calculation, corresponds to a different color. The red bars correspond to the case when there is no SE trapping in the plasmasphere via Coulomb collisional processes and no backscatter of the trapped SE energy from the plasmasphere ($\alpha = 1$; $\beta = 0$). Such a situation is represented in the FLIP model [*Young et al.*, 1980; *Richards et al.*, 1983, 2000], which calculates major and minor ion densities and ion and electron temperatures along closed magnetic field lines from 90 km in the northern hemisphere to 90 km in the

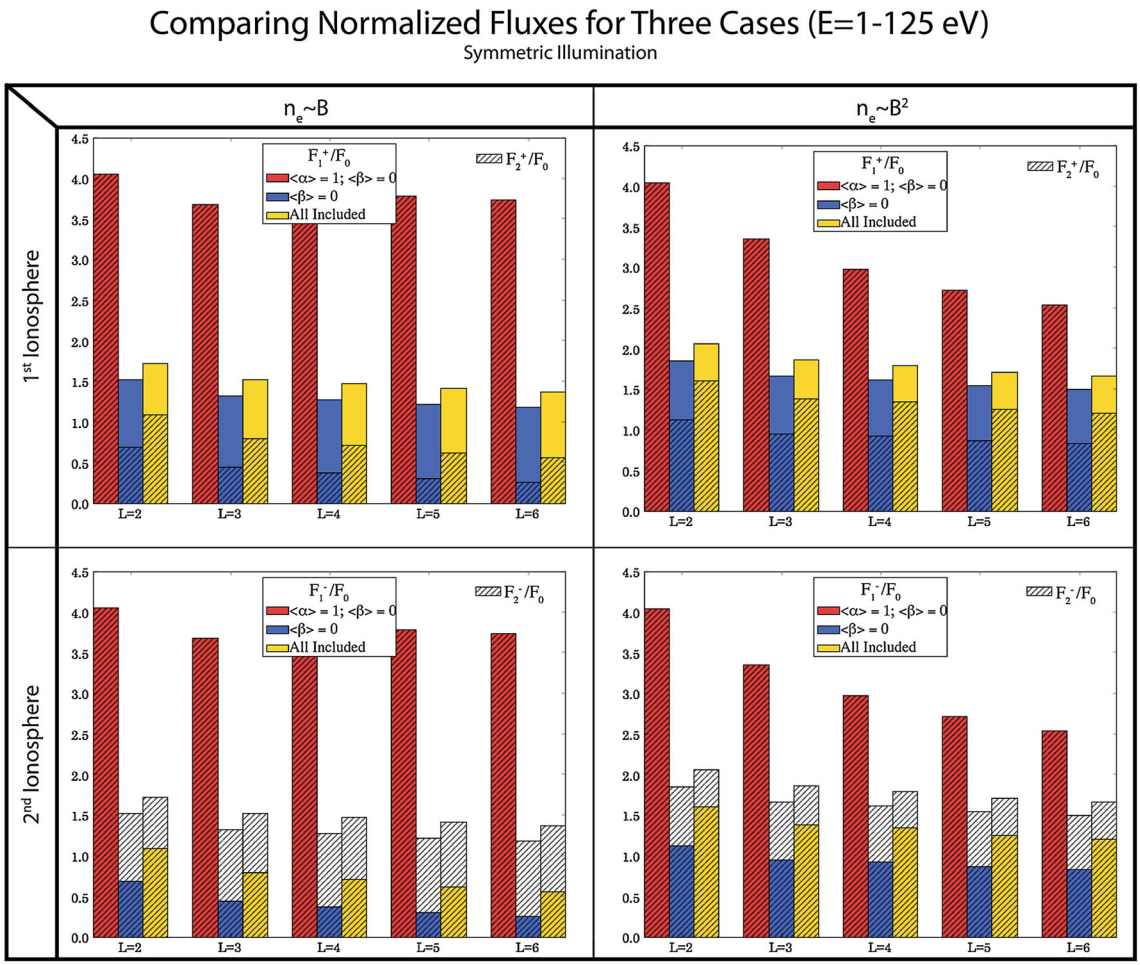

Figure 3. Normalized fluxes in each ionosphere for thermal electron density in the plasmasphere proporotional to B and B^2. Values for $L = 2$–6 are shown. Solid colors are the normalized flux in the first ionosphere, and dashed lines are the normalized flux in the second ionosphere.

conjugate hemisphere. The FLIP model includes an optimized two-stream photoelectron model [initially developed by *Banks and Nagy*, 1970] to efficiently calculate thermal electron heating and secondary ion production rates. The blue bars correspond to the case of $\beta = 0$, represented in the *Krinberg and Tashchilin* [1984] SE plasmaspheric energy deposition scenario when photoelectron plasmaspheric transparency had been found with an assumption of an infinite plasmaspheric trapped zone [*Khazanov et al.*, 1992]. In this case, electrons are allowed to scatter into the trapped zone but there is no return flux ("backscatter") from the trapped zone back into the loss cone.

[37] Looking at the calculated parameters for the above-mentioned two cases presented in this figure and comparing them to the case when all processes are included (the color yellow on Figures 3 and 4), we conclude that for some of the parameters that are shown in these figures, a robust, self-consistent description of SE transport in the ionosphere and plasmasphere is absolutely crucial. We also conclude that the contribution of the different backscattering processes in the ionospheric SE energy escape is a complicated function of L-shells and thermal plasma density distribution along geomagnetic field lines, emphasizing the necessity to consider the ionosphere and plasmasphere as one coupled system.

[38] As a consequence of these results, we infer that any simplification in the description of SE ionosphere-plasmasphere transport or disregard of some of the physical processes that form the SE distribution could lead to differences in calculations of the normalized SE flux by factors of 2 to 4. This implies that a self-consistent approach to SE ionosphere-plasmasphere transport produces significant changes in the SE energy exchange between the plasmasphere and the magnetically conjugate ionospheres compared with "pure" ionospheric or plasmaspheric calculations. For this reason, such an approach must be included in a future ionosphere-magnetosphere modeling network.

[39] Finally, let us discuss ionosphere-plasmasphere energy deposition processes. The plasmaspheric transparency presented by equation (12) was defined in terms of the ratio of unidirectional fluxes. Let as redefine this value in terms of the omnidirectional fluxes that are needed for energy deposition calculations. In this case, the plasmaspheric transparency will be given as

$$T_o = \left(F_1^- + F_2^+\right)/\left(F_1^+ + F_2^-\right) = 1 - \varepsilon. \tag{25}$$

and, based on equations (13)–(15), does not depend on the condition of illumination in the conjugate ionospheres. This result

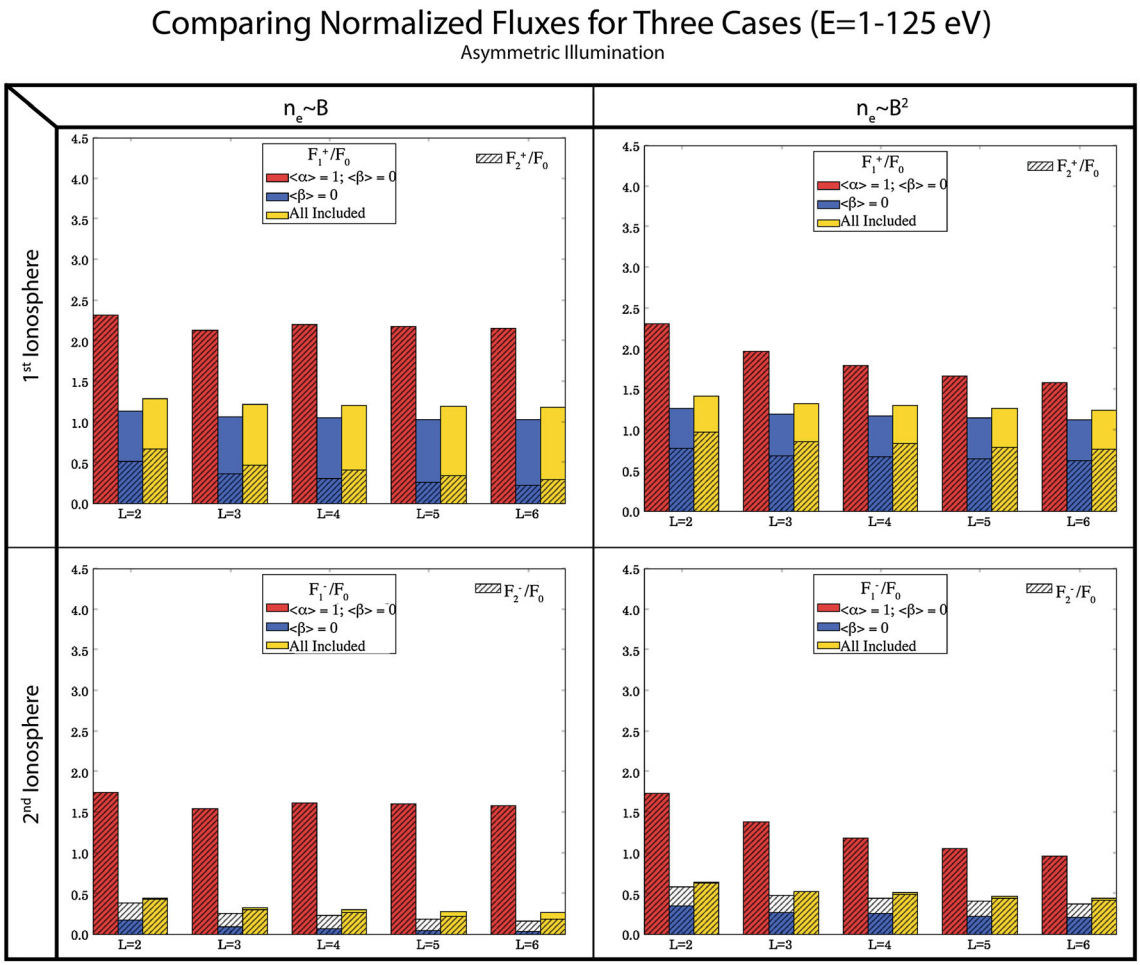

Figure 4. Normalized fluxes in each ionosphere for thermal electron density in the plasmasphere proporotional to B and B^2. Values for $L = 2$–6 are shown. Solid colors are the normalized flux in the first ionosphere, and dashed lines are the normalized flux in the second ionosphere.

is identical to the transparency calculation of equation (18) that was found through the unidirectional fluxes when illumination condition in the both ionospheres was the same. This means that the usage of plasmaspheric transparency in the energy deposition calculation as is defined by equation (18) and used by *Krinberg and Tashchilin* [1984] and do not represent properly the arbitrary condition of illumination in the conjugate ionospheres.

[40] Now let us compare the omnidirectional fluxes at the plasmaspheric boundaries in the conjugate ionosphere by introducing the following parameter, R,

$$R = \left(F_1^+ + F_1^-\right)/\left(F_2^+ + F_2^-\right). \tag{26}$$

Given the calculation of this ratio for the different condition of illumination in the conjugate ionospheres with the SE fluxes defined as equations (13)–(15), one can get the following relations

$$R_{\mathrm{sym}} = 1, \qquad R_{\mathrm{nsym}} = \alpha(1 + A + \beta A)/\left(1 + \beta + \alpha^2 A\right) \tag{27}$$

Because the omnidirectional SE fluxes determine the energy deposition to the thermal ionospheric electrons, even ionospheric nonlocal heating must be determined by taking into account ionosphere-plasmasphere SE transport. If, for example, in equation (27), $\alpha = 1$ and $\beta = 0$, coefficients that represent energy deposition calculation on the basis of the two-stream code, $R_{\mathrm{sym}}/R_{\mathrm{nsym}} = 1$. That means that the FLIP code not only *underestimates* plasmaspheric heating of the thermal electrons in the magnetosphere but also *overestimates* energy deposition of SE to the nonlocal heating of ionospheric plasma. Figure 5, presented in the same format as Figures 3 and 4 shows the results of R_{nsym} and R_{o}. Here, Ro is the omnidirectional flux ratio in the region I for the symmetric and nonsymmetric condition of illumination

$$\begin{aligned} Ro &= \left(F_1^+ + F_1^-\right)_{\mathrm{sym}}/\left(F_1^+ + F_1^-\right)_{\mathrm{nsym}} \\ &= (1 + \alpha A)(1 + \alpha + \beta)/\alpha(1 + A + \beta A) \end{aligned} \tag{28}$$

[41] These parameters are calculated for the different L-shells and thermal plasma distribution along the field lines. There are very clear quantitative differences between these parameters when different approaches to ionosphere-plasmasphere SE transport have been used. As one can notice, for the same ionospheric sources, the FLIP code does not depend on L-shell parameters and density distribution of the thermal plasma along the geomagnetic field lines. As we mentioned in the

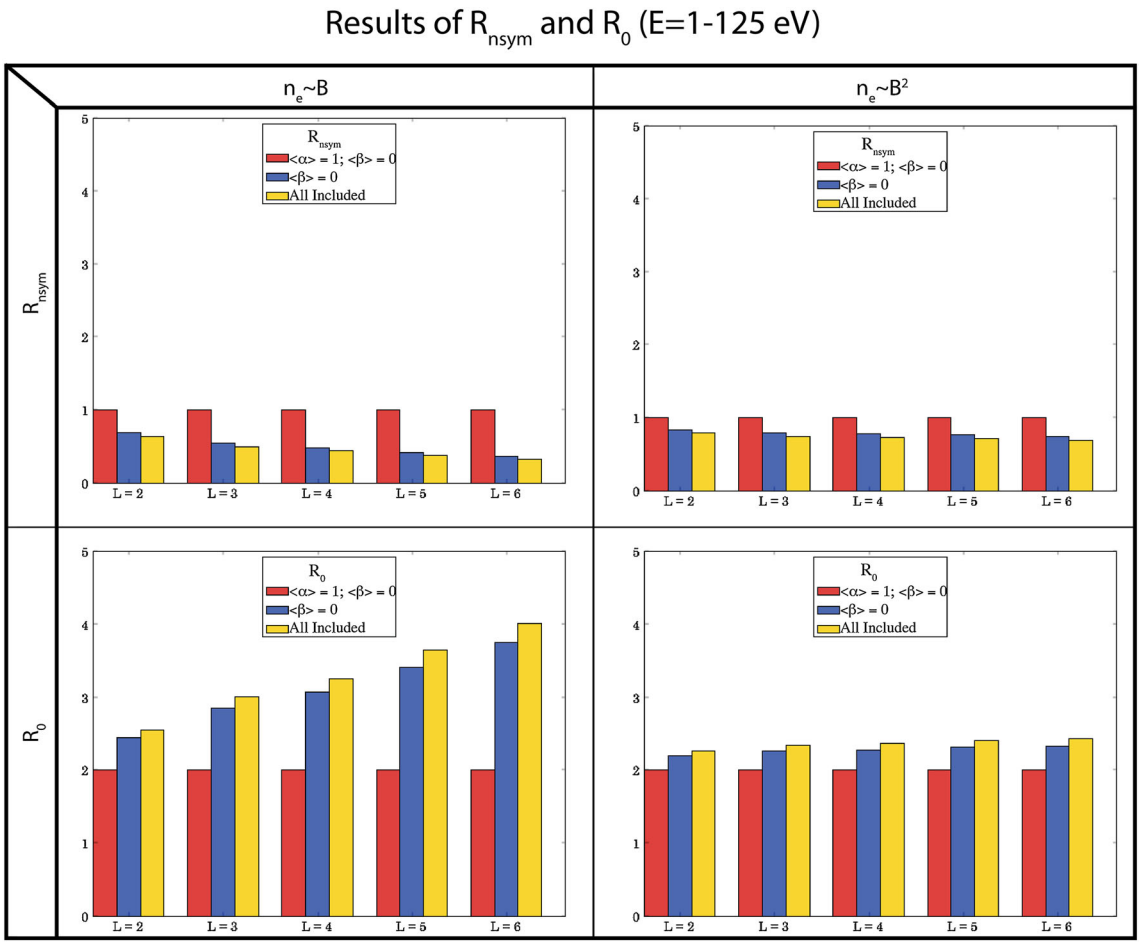

Figure 5. R_{nsym} and R_0 in each ionosphere for thermal electron density in the plasmasphere proporotional to B and B^2. Values for $L = 2$–6 arse shown.

introduction of this paper, this conclusion is consistent with work by *Richards and Peterson* [2008].

6. Conclusion

[42] This study presented a detailed, self-consistent calculation of SE transport along closed field lines in the inner magnetosphere. This approach was used to examine the quantities of plasmaspheric transparency, ionospheric albedo, magnetospheric trapping, and SE energy deposition to the thermal plasma. It was determined that the influence of pitch angle scattering by Coulomb collisions along the magnetic field line can be significant, although the SE mean free path is quite long, because the pitch angle width of the loss cone is very narrow near the equator and thus even small angle deflections will result in electron trapping.

[43] Because of this small but significant scattering process acting on the SEs as they traverse the plasmasphere from one ionosphere to the other, the amount of magnetospheric trapping varies as a function of L-shell, thermal plasma distribution along the field line, and solar illumination in the two conjugate ionospheres. As the field line length increases with L-shell, the magnetospheric trapping increases and the SE plasmaspheric transparency decreases. These effects, however, depend on the thermal plasma density distribution along the field line, with the effect being more pronounced along fully filled flux tubes than along depleted field lines undergoing plasmaspheric refilling (e.g., during and after magnetic storms). Interestingly, the SE plasmaspheric transparency also depends on ionospheric conditions. The solar illumination and ionospheric albedo change the upward SE flux leaving the ionosphere and entering the magnetospheric portion of the flux tube. Because the electrons can be backscattered multiple times, the conditions in both ionospheres play a key role in modulating the SE flux in the magnetosphere, therefore changing the total number of SE particles captured in the magnetospheric trap, which in turn affects the overall plasmaspheric transparency value (transparency increases with the upward ionospheric SE flux).

[44] It was found that the influence of these factors on SE plasmaspheric transparency could be significant. For the $L = 2$ field line, the energy-integrated (from 1 to 125 eV) plasmaspheric transparency can be as low as 0.455 and as high as 0.779, changing by nearly a factor of two. The range becomes larger at higher L-shells, however, with the $L = 6$ field line having a plasmaspheric transparency variation from 0.217 to 0.726, more than a factor of three difference. Therefore, it is concluded that the quantity of SE plasmaspheric transparency is a complicated function of many factors.

[45] We further used a phenomenological model to compare our kinetic approach, which includes all processes important to SE transport, with other approaches that do not fully account for all relevant processes. The comparison demonstrated that simplifications in the description of SE ionosphere-magnetosphere transport, or disregard of important physical processes such as pitch angle scattering, lead to differences in the normalized flux by factors of 2 to 4.

[46] The complex dependence of SE transport on multiple factors has implications for interpreting high-altitude electron measurements and for developing global coupled modeling networks. Because these electrons are a dominant heat source for the low and mid latitude ionosphere and are capable of traveling significant distances before depositing their energy, the processes of interhemispheric transport and nonlocal heating are critical to accurately predicting a wide array of geospace quantities. Thus, SE transport should be robustly and self-consistently calculated within the ionosphere-magnetosphere system with a model that accurately resolves the scattering, trapping, and interplay of particles along the field lines between the conjugate ionospheric regions.

[47] **Acknowledgments.** This material is based on work supported by the National Aeronautics and Space Administration SMD/Heliophysics Supporting Research program for Geospace SR&T. The authors would like to thank the reviewers for their useful comments.

References

Banks, P. M., and A. F. Nagy (1970), Concerning the influence of elastic scattering upon photoelectron transport and escape. *J. Geophys. Res.*, *75*, 1902–1910.

Bell, K. L., and R. P. Stafford (1992), Photoionization cross sections for atomic oxygen. *Planet. Space Sci.*, *40*, 1419–1424.

Bilitza, D. (1990), Progress report on IRI status. *Adv. Space Res.*, *10*(11), 3–5.

Buonsanto, M. J., M. Codrescu, B. A. Emery, C. G. Fesen, T. J. Fuller-Rowell, D. J. Menendez-Alvira, and D. P. Sipler (1997), Comparison of models and measurements at Millstone Hill during the January 24–26, 1993, minor storm interval, *J. Geophys. Res.*, *102*, 7267.

Chamberlin, P. C., T. N. Woods, and F. G. Eparvier (2007), Flare Irradiance Spectral Model (FISM): Daily component algorithms and results, *Space Weather*, *5*, S07005, doi:10.1029/2007SW000316.

Chamberlin, P. C., T. N. Woods, and F. G. Eparvier (2008), Flare Irradiance Spectral Model (FISM): Flare component algorithms and results, *Space Weather*, *6*, S05001, doi:10.1029/2007SW000372.

Conway, R. R. (1988), Photoabsorption and photoionization cross sections: A compilation of recent measurements. Memo Rep. *6155*, Nav. Res. Lab., Washington, D.C.

Fennelly, J. A., and D. G. Torr (1992), Photoionization and photoabsorption cross sections of O, N_2, O_2, and N for aeronomic calculations, *At. Data Nucl. Data Tables*, *51*, 321–363.

Galperin, Y. I., and T. M. Mulyarchik (1966), On the height distribution of photoelectrons. *Kosmich. Issledov. 4*, 932–941 (in Russian).

Gastman, I. J. (1973), Theoretical investigation and plasma line measurements of conjugate photoelectrons in the ionosphere. Ph. D. Thesis. Univ. of Michigan, Ann Arbor.

Hedin, A. E. (1991), Extension of the MSIS thermospheric model into the middle and lower atmosphere, *J. Geophys. Res.*, *96*, 1159–1172.

Hinteregger, H. E. (1981), Representations of solar EUV fluxes for aeronomical applications. *Adv. Space Res.*, *1*, 39–52.

Huba, J. D., G. Joyce, and J. A. Fedder (2000), SAMI2 is another model of the ionosphere (SAMI2): A new low-latitude ionosphere model, *J. Geophys. Res.*, *105*(A10), 23,035.

Khazanov, G. V. (1979), *The Kinetics of the Electron Plasma Component of the Upper Atmosphere* (in Russian), Moscow, Nauka, English translation: Washington, D.C., National Translation Center, #80-50707, 1980.

Khazanov, G. V. (2011), *Kinetic Theory of the Inner Magnetospheric Plasma*, Springer, New York Heidelberg Dordrecht London.

Khazanov, G. V., T. I. Gombosi, A. F. Nagy, and M. A. Koen (1992), Analysis of the ionosphere-plasmasphere transport of superthermal electrons: 1. Transport in the plasmasphere, *J. Geophys. Res.*, *97*, 16,887–16,895.

Khazanov, G. V., and M. W. Liemohn (1995), Nonsteady state ionosphere-plasmasphere coupling of superthermal electrons, *J. Geophys. Res.*, *100*, 9669.

Khazanov, G. V., and M. W. Liemohn (2000), Kinetic theory of superthermal electron transport, in *Recent Research Developments in Geophysics*, 3 (part 2), edited by S. G. Pandalai, pp. 181–201, Research Signpost, Trivandrum, India.

Khazanov, G. V., and M. W. Liemohn (2002), Transport of photoelectrons in the nightside magnetosphere, *J. Geophys. Res.*, *107*(A5), 1064, doi:10.1029/2001JA000163.

Khazanov, G. V., M. A. Koen, Y. V. Konikov, and I. M. Sidorov (1984), Simulation of ionosphere-plasmasphere coupling taking into account ion inertia and temperature anisotropy. *Planet. Space Sci.*, *32*, 585–598.

Khazanov, G. V., T. Neubert, and G. D. Gefan (1994), A unified theory of ionosphere-plasmasphere transport of suprathermal electrons. *IEEE Trans. Plasma Sci.*, *22*, 187–198.

Khazanov, G. V., T. E. Moore, M. W. Liemohn, V. K. Jordanova, and M.-C. Fok (1996), Global collisional model of high-energy photoelectrons, *Geophys. Res. Lett.*, *23*, 331.

Khazanov, G. V., M. W. Liemohn, J. U. Kozyra, and T. E. Moore (1998), Inner magnetospheric superthermal electron transport: Photoelectron and plasma sheet electron sources, *J. Geophys. Res.*, *103*, 23,485.

Khazanov, G. V., M. W. Liemohn, J. U. Kozyra, and D. L. Gallagher (2000), Global energy deposition to the topside ionosphere from superthermal electrons, *J. Atmos. Solar-Terr. Phys.*, *62*, 947.

Krinberg, I. A., and G. K. Matafonov (1978), Coulomb collision-induced photoelectron trapping by the geomagnetic field and electron gas heating in the plasmasphere. *Ann. Geophys.*, *34*, 89–96.

Krinberg, and Tashchilin (1984), Ionosphere and Plasmasphere, Publish House, Nauka (in Russian).

Lejeune, J., and F. Wormser (1976), Diffusion of photoelectrons along a field line inside the plasmasphere. *J. Geophys. Res. 81*, 2900–2916.

Lejeune, J. (1978), "Two-stream" photoelectron distributions with interhemispheric coupling: A mixing of analytical and numerical methods, *Planet. Space Sci.* 561–576.

Liemohn, M. W., and G. V. Khazanov (1998), Determining the significance of electrodynamic coupling between superthermal electrons and thermal plasma, in Geospace Mass and Energy Flow, *Geophys. Monogr. Ser.*, vol. 104, edited by J. L. Horwitz, D. L. Gallagher, and W. K. Peterson, p. 343, AGU, Washington, D. C.

Liemohn, M. W., J. L. Fox, A. F. Nagy, and X. Fang (2004), Hot carbon densities in the exosphere of Venus, *J. Geophys. Res.*, *109*, A10307, doi:10.1029/2004JA010643.

Nagy, A. F., and P. M. Banks (1970), Photoelectron fluxes in the ionosphere. *J. Geophys. Res.*, *75*, 6260–6270.

Newberry, I. T., R. H. Comfort, P. G. Richards, and C. R. Chappell (1989), Thermal He^+ in the plasmasphere: Comparison of observations with numerical calculations, *J. Geophys. Res.*, *94*, 15,265–15,276.

Peterson, W. K., J. P. Doering, T. A. Potemra, R. W. McEntire, and C. O. Bostrom (1977), Conjugate photoelectron fluxes observed on Atmosphere Explorer C, *Geophys. Res. Lett.*, *4*, 109.

Richards, P. G., and W. K. Peterson (2008), Measured and modeled backscatter of ionospheric photoelectron fluxes, *J. Geophys. Res.*, *113*, A08321, doi:10.1029/2008JA013092.

Richards, P. G., R. W. Schunk, and J. J. Sojka (1983), Large-scale counter streaming of H^+ and He^+ along plasmaspheric flux tubes, *J. Geophys. Res.*, *88*, 7879–7886.

Richards, P. G., et al. (2000), On the relative importance of convection and temperature on the behavior of the ionosphere in North America during January 6–12, 1997, *J. Geophys. Res.*, *105*(A6), 12,763–12,776.

Sanatani, S., and W. B. Hanson (1970), Plasma temperature in the magnetosphere. *J. Geophys. Res.*, *75*, 769–775.

Solomon, S. C., P. B. Hays, and V. J. Abreu (1988), The auroral 6300 Å emission: Observations and modeling. *J. Geophys. Res.*, *93*, 9867–9882.

Takahashi, T. (1973), Energy degradation and transport of photoelectrons escaping from the upper ionosphere. *Rept. Ionos. Space Res. Jap. 27*, 79–86.

Varney, R. H., W. E. Swartz, D. L. Hysell, and J. D. Huba (2012), SAMI2-PE: A model of the ionosphere including multistream interhemispheric photoelectron transport, *J. Geophys. Res.*, *117*, A06322, doi:10.1029/2011JA017280.

Woods, T. N., S. M. Bailey, W. K. Peterson, H. P. Warren, S. C. Solomon, F. G. Eparvier, H. Garcia, C. W. Carlson, and J. P. McFadden (2003), Solar extreme ultraviolet variability of the X-class flare on 21 April 2002 and the terrestrial photoelectron response, *Space Weather*, *1*(1), 1001, doi:10.1029/2003SW000010.

Young, E. R., P. G. Richards, and D. G. Torr (1980), A flux preserving method of coupling first and second order equations to simulate the flow of plasma between the protonosphere and the ionosphere, *Comput. Phys.*, *38*, 141–156.